

# Structural Characterization of Novel Styrene–Butadiene Block Copolymers Containing Syndiotactic Styrene Homosequences

Michela Caprio,<sup>†</sup> Maria Cristina Serra, Daniel E. Bowen,<sup>‡</sup> and Alfonso Grassi\*

Dipartimento di Chimica, Università di Salerno, via S. Allende, I-84081 Baronissi, Italy

Received June 27, 2002; Revised Manuscript Received September 17, 2002

**ABSTRACT:** Samples of poly(syndiotactic styrene-*co*-butadiene) (SPS-B) have been prepared using methylalumoxane (MAO) activated CpTiCl<sub>3</sub> under a range of experimental conditions. Copolymerization activities were low (24–36 kg mol<sup>-1</sup> of cat. h<sup>-1</sup>) and nearly constant over the range of polymerization temperatures investigated (25–70 °C). Eight sPS-B samples were synthesized at 25 °C with styrene molar fractions ( $x_s$ ) covering a full range of compositions ( $x_s = 0.15$ – $0.92$ ). The copolymer samples were characterized by solution and solid state <sup>13</sup>C NMR spectroscopy, X-ray powder diffraction analysis, and thermal (DSC) analysis. The <sup>13</sup>C NMR analysis of the copolymer microstructure suggests that the butadiene homosequences are primarily *cis*-1,4 and the styrene segments are syndiotactic. However, some 1,2- and *trans*-1,4-butadiene units are occasionally formed during the polymerization process. The <sup>13</sup>C NMR resonances diagnostic of the monomer triads comprising styrene units (SSB, SBS, BBS, BSB, and SSS) were assigned and the average styrene block lengths ( $n_s$ ) calculated. Copolymer samples in which  $n_s > 9$  are crystalline due to the syndiotactic polystyrene segments detected in the  $\delta$ -toluene clathrate form with melting points in the range 205–230 °C. Syndiotactic polystyrene segments with shorter styrene block lengths are amorphous and partially included in the poly(butadiene) rubber domains. TEM images of sample **13** ( $x_s = 0.37$ ,  $n_s = 8.8$ ) show the presence of small sPS fibers.

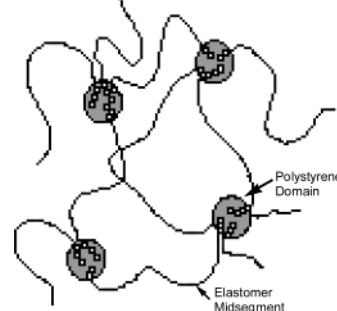
## Introduction

Styrene–butadiene diblock (SB) and triblock (SBS) copolymers are thermoplastic elastomers of the general type AB and ABA. A variety of SB and SBS copolymers are manufactured commercially in large volumes with a high degree of control over the block length, molecular weight, and microstructure using well-understood anionic polymerizations.<sup>1</sup> At moderate temperatures, these types of copolymers adopt one of the four following phase-separated morphologies: spheres, cylinders, double gyroid, and lamellae.<sup>2</sup> The phase morphology is dictated primarily by the copolymer composition, with the styrene content and the molecular weight of the styrene homosequences (typical range 10 000–17 000 amu) being particularly important. The thermodynamic stability of the different morphologies has been thoroughly investigated, both theoretically and experimentally,<sup>3</sup> and the different structures have been monitored by TEM (transmission electron microscopy).<sup>4</sup>

Styrene–butadiene thermoplastic elastomers generally consist of hard, phase-separated styrenic domains tethered by soft, elastomeric poly(butadiene) segments.<sup>5</sup> At temperatures below the glass transition temperature ( $T_g$ ) of the polystyrene homosequences, the phase-separated styrene domains act like physical cross-links. These physical cross-links impart resilience, tensile strength, and abrasion resistance to the copolymers in the uncured state.

A unique feature of these materials is the thermoreversible nature of the styrenic physical cross-links. The glass transition temperature of polystyrene segments in typical SB and SBS copolymers is  $\sim 100$  °C.<sup>6</sup> Above

Scheme 1



this temperature the hard styrene domains soften, thus allowing the material to flow under low shear. Conversely, when the material cools, the styrene homosequences reaggregate and phase-separate. This combination of properties provides the cured-like behavior and melt processability, below and above  $\sim 100$  °C, respectively.

A number of styrene–butadiene block copolymers other than SB and SBS have been synthesized using known anionic polymerization techniques. These include multiblock and graft copolymers of the general (AB)<sub>*n*</sub> type.<sup>7</sup> However, compared to SB and SBS block copolymers, the phase morphologies of these materials are complicated and not easily predicted.<sup>6</sup> In general, poly(styrene-*block*-butadiene) copolymers synthesized anionically contain isolated styrene units or atactic styrene homosequences.<sup>8–10</sup> Copolymers containing stereoregular styrene sequences, although of great interest, were not available until recently. Poly(styrene-*block*-butadiene) copolymers possessing crystalline, stereoregular polystyrene domains should exhibit unique properties compared to similar copolymers with atactic styrene homosequences. Copolymers containing high melting stereoregular styrene blocks may be more thermally stable, have harder phase-separated styrenic domains, and improved mechanical properties and processing.

<sup>†</sup> Current address: Pirelli Pneumatici s.p.a., viale Sarca 222, 20131 Milano Italy.

<sup>‡</sup> The Goodyear Tire & Rubber Company, 1144 East Archwood Avenue, Akron, OH 44316.

\* To whom correspondence should be addressed. E-mail: agrassi@unisa.it.

**Table 1. sPS–B Copolymers (1–6) and sPS and PBD Samples Prepared at Different Polymerization Temperatures (15–70 °C) Using the CpTiCl<sub>3</sub>/MAO Catalyst in Toluene**

sample	temp (°C)	yield (g)	copolymer composition (mol %)
<b>1<sup>a</sup></b>	15	0.23	$x_S = 0.43$ ; $x_B = 0.50$ ; $x_V = 0.07$
<b>2<sup>a</sup></b>	25	1.00	$x_S = 0.50$ ; $x_B = 0.43$ ; $x_V = 0.07$
<b>3<sup>a</sup></b>	35	1.20	$x_S = 0.66$ ; $x_B = 0.27$ ; $x_V = 0.07$
<b>4<sup>a</sup></b>	45	1.24	$x_S = 0.40$ ; $x_B = 0.53$ ; $x_V = 0.07$
<b>5<sup>a</sup></b>	55	1.20	$x_S = 0.60$ ; $x_B = 0.33$ ; $x_V = 0.07$
<b>6<sup>a</sup></b>	70	1.23	$x_S = 0.50$ ; $x_B = 0.46$ ; $x_V = 0.04$
<b>7<sup>b</sup></b>	25	4.00	$x_S = 1$
<b>8<sup>b</sup></b>	70	16.00	$x_S = 1$
<b>9<sup>c</sup></b>	25	4.00	$x_B = 1$
<b>10<sup>c</sup></b>	70	8.00	$x_B = 1$

<sup>a</sup> The copolymerization runs were conducted according to the procedure described in the Experimental Section. <sup>b</sup> Styrene homopolymerization was conducted under the following conditions: 100 mL of toluene, 75 mL of styrene,  $3.5 \times 10^{-5}$  mol of CpTiCl<sub>3</sub>, 0.60 g of MAO (Al/Ti molar ratio = 400). <sup>c</sup> Butadiene homopolymerization was conducted under the following conditions: 0.60 g of MAO (Al/Ti molar ratio = 400) was added to 150 mL of toluene and the solution equilibrated with a gas mixture containing 15% v/v of butadiene in nitrogen flowing at 700 mL/min. Polymerization was started by injecting 2 mL of a toluene solution of CpTiCl<sub>3</sub> ( $3.5 \times 10^{-5}$  mol).

We succeeded in obtaining styrene–butadiene block copolymers containing syndiotactic styrene homosequences (sPS–B) using a number of MAO activated titanium compounds, namely CpTiX<sub>3</sub> (Cp = C<sub>5</sub>H<sub>5</sub>, X = Cl, F; Cp = C<sub>5</sub>Me<sub>5</sub>, X = Me) and TiX<sub>n</sub> ( $n = 3$ , X = acetylacetonate (acac);  $n = 4$ , X = O<sup>t</sup>Bu).<sup>11</sup> Of the catalyst systems studied, CpTiCl<sub>3</sub>/MAO showed the highest activity (polymerization temperature = 15 °C). The reactivity ratios product ( $r_1 r_2 = 400$ ), evaluated using the Finemann–Ross method, suggest a blocky composition of the copolymer product, which was confirmed by ozonolysis and DSC analysis. The butadiene concentration in the monomer feed was critical in controlling the level of styrene incorporated in the copolymer and for the formation of syndiotactic styrene homosequences: e.g., at high butadiene concentration in the feed a partial poisoning of the catalyst occurs, and a mixture of atactic polystyrene and polybutadiene was recovered from the copolymerization process.<sup>11</sup> The butadiene molar fraction in the monomer feed could not be accurately measured, and the samples were therefore typically rich in butadiene. Now we are able to report on the synthesis of sPS–B samples covering a full range of monomer compositions and the results of our preliminary investigation of the microstructure and morphology of these materials.

## Results and Discussion

**Synthesis of the sPS–B Copolymers.** Styrene–butadiene copolymerizations were investigated over a range of temperatures (15–70 °C) using CpTiCl<sub>3</sub>/MAO in order to determine the conditions needed for high polymerization activity (Table 1; **1–6**). The butadiene molar fraction in the gas phase was measured using a mass flow controller, with the inlet and outlet gas mixture compositions being monitored by GC analysis (see Experimental Section). The polymerization experiments maintained similar butadiene concentrations at each temperature tested. By calibrating the butadiene concentration in the monomer feed streams, copolymers with nearly the same styrene molar fraction ( $x_S = 0.40$ – $0.66$ ) were produced. The polymerization activities, based on polymer yields, increased with increasing

temperature from 15 to 25 °C but plateaued in the 25–70 °C temperature range (Table 1). Considering that both styrene and butadiene homopolymerization rates abruptly increase with temperature (Table 1, **7–10**), it is surprising that styrene–butadiene copolymerization yields appear to be independent of temperature above 25 °C. If the copolymerization rates depend on the sum of the homopolymerization and mixed kinetic constants ( $k_{SS}$ ,  $k_{BB}$ ,  $k_{BS}$ , and  $k_{SB}$ ) and the homopolymerization yields of both styrene and butadiene are higher than copolymerization yields under comparable conditions (see entries 7 and 9), then this behavior seems quite unusual and may be related to the specific copolymerization mechanism.<sup>11</sup>

**<sup>13</sup>C NMR Characterization of the sPS–B Copolymers.** Eight samples of sPS–B (Table 2, **11–18**) with styrene molar fractions ( $x_S$ ) covering a full range of composition ( $x_S = 0.15$ – $0.92$ ) were prepared at 25 °C. In all explored conditions (e.g., runs **11–18**) the monomer conversion is always rather low, and the productivity of the catalyst is in the range 24–36 kg mol<sup>−1</sup> mol of cat. h<sup>−1</sup>.

The microstructures of the sPS–B copolymers are complicated by the presence of four monomer units, namely 1,2-vinyl (V), *cis*-1,4 (C), *trans*-1,4 (T) butadiene, and styrene (S). This produces at least 10 monomer diads (CV, CC, CS, CT, VV, TV, SV, SS, TS, and TT). Moreover, splitting of the SS and VV diad resonances because of stereochemical effects (isotactic or syndiotactic arrangement) and monomer enchainment (head-to-head or tail-to tail) must also be considered. Furthermore, the regiochemistry of V and S insertion would produce inequivalent BS and BV diads (where B is a 1,4-butadienyl unit regardless of the *cis* or *trans* stereochemistry of the double bond). Assignment of the <sup>13</sup>C NMR triad resonances is, of course, much more difficult. Several authors have previously reported the <sup>13</sup>C NMR characterization of SBR.<sup>8–10</sup> Sato et al. made assignments at the triad level using low molecular weight copolymers and properly deuterated model compounds.<sup>10</sup> These authors also reported incremental shift factors for the methylene carbons in the  $\alpha$ -,  $\beta$ -, and  $\gamma$ -position from the 1,2-vinyl (V), styrenyl (S), and *cis* (C) or *trans* (T) 1,4-butenyl units in a polymethylene chain. Stereochemical effects of the SS, SV, and VV diads were also considered.<sup>12</sup> On the basis of these results, we analyzed the microstructure of the sPS–B copolymers, focusing our attention on the <sup>13</sup>C NMR signals diagnostic of the monomer triads comprising S units. Under the conditions tested, the CpTiCl<sub>3</sub>/MAO catalyst system promotes the highly regiospecific insertion of styrene<sup>13</sup> and 1,2-butadiene,<sup>14,15</sup> with both occurring exclusively in a secondary or 2,1-fashion. The catalyst system also promotes the highly syndiospecific polymerization of styrene.<sup>16</sup>

The chemical shifts of the <sup>13</sup>C NMR signals diagnostic of the different monomer triads are listed (Table 3) for the aliphatic region. The assignments are also displayed (Figure 1). The patterns of the resonances attributed to the carbons of the same triad have equal relative intensities in all the samples analyzed, confirming the assignments.

Inspection of the <sup>13</sup>C NMR spectra of three sPS–B copolymers covering the full range of compositions (Figure 2; **18**,  $x_S = 0.92$ ; **14**,  $x_S = 0.55$ ; **11**,  $x_S = 0.15$ ) helps in accounting for the assignments listed in Table 3. The <sup>13</sup>C NMR spectrum of sample **18** ( $x_S = 0.92$ )

Table 2. Physical Properties of the sPS–B Samples 11–18

sample	copolymer composition in diads (molar fraction) <sup>a</sup>	copolymer composition (monomer molar fraction) <sup>b</sup>	av monomer block lengths <sup>c</sup>	$T_m^d$ (°C)	$T_g$ (°C)	yield (g)
11	SS = 0.19	$x_S = 0.15$	$n_S = 5.8$		–95	1.30
	SB + BS = 0.05	$x_B = 0.73$				
	BB = 0.76	$x_V = 0.12$				
12	SS = 0.29	$x_S = 0.29$	$n_S = 8.3$		–90	1.20
	SB + BS = 0.04	$x_B = 0.64$				
	BB = 0.67	$x_V = 0.07$				
13	SS = 0.36	$x_S = 0.37$	$n_S = 8.8$		–80	1.00
	SB + BS = 0.04	$x_B = 0.55$				
	BB = 0.59	$x_V = 0.07$				
14	SS = 0.44	$x_S = 0.55$	$n_S = 9.0$		–80	0.98
	SB + BS = 0.06	$x_B = 0.38$				
	BB = 0.48	$x_V = 0.07$				
15	SS = 0.60	$x_S = 0.65$	$n_S = 12$	205	n.d.	1.25
	SB + BS = 0.06	$x_B = 0.29$				
	BB = 0.33	$x_V = 0.06$				
16	SS = 0.70	$x_S = 0.70$	$n_S = 13$	210	n.d. <sup>f</sup>	1.30
	SB + BS = 0.06	$x_B = 0.24$				
	BB = 0.24	$x_V = 0.06$				
17	SS = 0.75	$x_S = 0.82$	$n_S = 17$	224	n.d. <sup>f</sup>	1.20
	SB + BS = 0.04	$x_B = 0.11$				
	BB = 0.20	$x_V = 0.07$				
18	SS = 0.85	$x_S = 0.92$	$n_S = 50$	230	n.d. <sup>f</sup>	1.25
	SB + BS = 0.05	$x_B = 0.03$				
	BB = 0.09	$x_V = 0.05$				

<sup>a</sup> S = styrene; B = 1,2- and 1,4-butadiene. <sup>b</sup> The styrene, 1,4-butadiene, and 1,2-butadiene molar fractions,  $x_S$ ,  $x_B$ , and  $x_V$ , respectively, were determined by integrating the appropriate <sup>1</sup>H NMR resonances (see Experimental Section). <sup>c</sup> The average block lengths were calculated according to the calculations and equations reported in the Appendix. <sup>d</sup> Melting points of the sPS segments determined by DSC analysis. For comparison, the melting points of the high and low molecular weight sPS are 270 and 250 °C, respectively. <sup>e</sup> Glass transition temperatures of the PBD segments. The values for samples 15–18 containing short PBD segments cannot be exactly identified because of the low intensity of the signal due to the phase transition. For comparison, the  $T_g$  of PBD is 95 °C. <sup>f</sup> Not determined.

exhibits resonances corresponding to the syndiotactic polystyrene triad SSS (lines 4 and 14 of Table 3) corresponding to the SS<sub>1</sub>S and SS<sub>2</sub>S carbons, respectively. These resonances are at the same chemical shifts in sPS homopolymer.<sup>16</sup> The monomer triads comprising one B unit are oriented producing inequivalent SSB and BSS sequences. The <sup>13</sup>C NMR signals diagnostic for the SSC triad are SS<sub>1</sub>C (line 7), SS<sub>2</sub>C (line 9), and SSC<sub>1</sub> (line 25). The reverse CSS triad is characterized by lines 10 and 17, corresponding to the CS<sub>2</sub>S and CS<sub>1</sub>S carbons, respectively. The chemical shifts of spectral lines 7, 9, 10, and 17 were assigned after that the corresponding chemical shifts were calculated using the following general method. The <sup>13</sup>C NMR signals of the methylene (S<sub>1</sub>) and aliphatic methine (S<sub>2</sub>) of the styrene units, observed in the syndiotactic styrene–poly(ethylene) copolymers (sPS–PE) at 41.4 and 44.2 ppm,<sup>15</sup> were assumed as reference values, and the desired chemical shift was calculated using the additive shift factors proposed by Sato et al.<sup>10</sup> and Beebe<sup>17</sup> for the methylene carbons in a given position from the C unit. The same procedure was used successfully to calculate the chemical shifts of the SS<sub>1</sub>T and SS<sub>2</sub>T carbons (Table 3; lines 6 and 8, respectively), which were expected at 43.3 and 43.4 ppm. The  $\Delta\delta$  between lines 8 (SS<sub>2</sub>T) and 9 (SS<sub>2</sub>C) agrees with the chemical shift difference expected on the basis of the shift factors reported by Sato<sup>10</sup> for the B units with trans and cis stereochemistry, confirming the validity of the method we used. The SSV and VSS sequences are scarcely probable events, and the corresponding signals should overlap those of the SSS triad. The CSC triad is characterized by lines 1, 19, 21, and 31, corresponding to the CS<sub>2</sub>C, CS<sub>1</sub>C, CSC<sub>1</sub>, and CSC<sub>4</sub> triads, respectively. The chemical shifts of the latter resonances appear at the same values observed by Sato et al. in the SBR copolymers.<sup>10</sup> The relative intensities of these resonances are low in the spectrum of sample

18 but increase in the spectrum of samples 14 and 11 where the concentration of styrene is lower and the probability of observing isolated styrene unit is higher (Figure 2). Signals corresponding to T<sub>4</sub>S, expected at 30.4 ppm, were not detected, whereas the ST<sub>1</sub> resonances are observed at 41.3 and 40.2 ppm, corresponding to the r-SST<sub>1</sub> and CST<sub>1</sub> triads.

The <sup>13</sup>C NMR signals expected for the poly(butadiene) (PBD) segments of the sPS–B samples are similar to those of SBR. The intensity of the <sup>13</sup>C NMR signals at 27.4 ppm, attributed to the CC<sub>1</sub>C and CC<sub>4</sub>C carbons, suggests that the butadiene homosequences are primarily *cis*-1,4. However, some V or T units are occasionally formed. The molar fraction of the V units is always rather low (see Table 2), roughly corresponding to ~11 mol % of the total butadiene fraction. The vinyl content also appears to be independent of copolymer composition, but it is lower than that in homo-PBD samples produced using the same catalyst system. The V units are isolated in the polymer chain. Signals diagnostic of the VV diads, expected in the region of the unsaturated carbons at 142.9 ppm and corresponding to the V<sub>3</sub>V carbons, are not detected even at high butadiene molar fractions.<sup>17,18</sup> Recent results on the characterization of anionic PBD samples containing similar vinyl content confirm that the formation of the VV diad is a scarcely probable event.<sup>19</sup> In the sPS–B copolymers isolated V units are observed in the SVS (lines 2 and 3), CVC (lines 5, 20, 23, and 36), and CVT (line 16) sequences. Monomer triads including V were also identified in VCV (lines 13, 18, 22, and 37) and CCV (lines 27 and 36) triads.

The molar concentration of T units in the sPS–B copolymers is quite similar to that in the PBD samples prepared with CpTiCl<sub>3</sub>/MAO under similar conditions. The presence of <sup>13</sup>C NMR resonances at 32.5 ppm (line 24), corresponding to the CT and TC sequences, con-



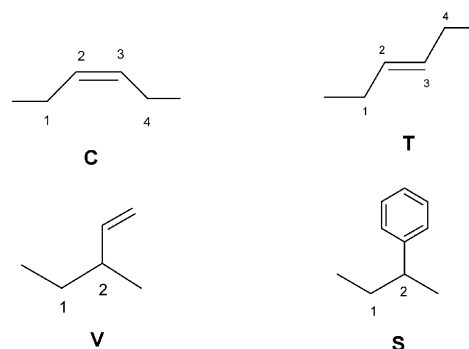
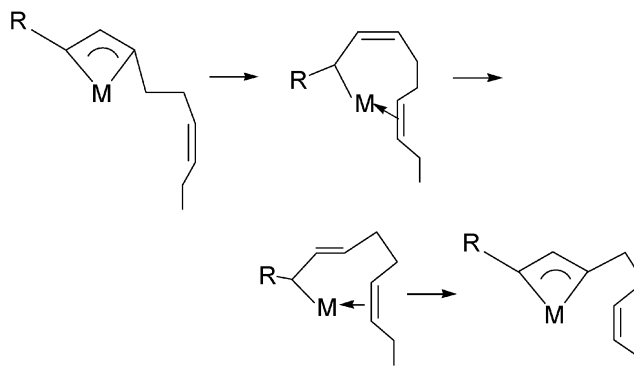
**Table 3. Selected  $^{13}\text{C}$  NMR Chemical Shifts Determined for the Monomer Triads in the sPS-B Copolymer Produced with  $\text{CpTiCl}_3/\text{MAO}$** 

line	sequence <sup>a</sup>	calcd chemical shifts (ppm) <sup>b</sup>	exptl chemical shifts (ppm)	ref
1	$\text{CS}_2\text{C}$	45.63–46.04	45.7	9
2	$\text{SVS}_1$	41–47	44.7	9
3	$\text{S}_1\text{VS}$	41–47	44.6	9
4	$\text{SS}_1\text{S}$	43.9	43.9	14 <sup>c</sup>
	$\text{SS}_1\text{V}^c$			
5	$\text{CV}_2\text{C}$	43.9–44.3	43.7	9
6	$\text{SS}_1\text{T}$	43.3	n.d.	<i>c</i>
7	$\text{SS}_1\text{C}$	43.7	43.5	<i>c</i>
8	$\text{SS}_2\text{T}$	43.4	n.d.	<i>c</i>
9	$\text{SS}_2\text{CC}$	42.92–43.47	43.3	<i>c</i>
10	$\text{CS}_2\text{S}$	42.46–43.18	42.8	<i>c</i>
11	$\text{CSV}_1$	39–42	42.6	9
12	$\text{SV}_1\text{S}$	39–42	42.2	9
13	$\text{VCV}_2$	40.6	40.7	9
14	$\text{SS}_2\text{S}$	40.6	40.6	14
15	$\text{CST}_1$	40.2	40.2	9
16	$\text{CVT}_1$	38.2	38.2	9
17	$\text{CS}_1\text{S}$	37.98–38.12	37.35	<i>c</i>
	$\text{CS}_1\text{V}$			
18	$\text{SCV}_1$	35.4–35.5	35.8	9
	$\text{VCV}_1$			
19	$\text{CS}_1\text{C}$	35.42–35.51	35.7	9
20	$\text{CV}_1\text{C}$	35.2–35.3	34.26	9
21	$\text{CSC}_1$	34.68	34.09	9
22	$\text{VC}_1\text{V}$	33.4	33.4	15
23	$\text{CVC}_1$	32.73	32.66	9
24	$\text{CT}_1$	32.7–33.88	32.5	9
	$\text{T}_4\text{C}$			
25	$\text{VSC}_1$	33.39–33.50	32.4	9 <sup>c</sup>
	$\text{SSC}_1^c$			
26	$\text{SSC}_4\text{C}$	27.32–27.44	27.38 (nr)	<i>c</i>
27	$\text{CC}_1\text{V}$	27.32–27.44	27.38 (nr)	9
28	$\text{VC}_4\text{C}$	27.32–27.44	27.38 (nr)	9
29	$\text{CC}_1\text{C}, \text{CC}_4\text{C}$	27.32–27.44	27.38 (nr)	9
30	$\text{CC}_1\text{SC}$	27.45	27.5 (nr)	9
31	$\text{CSC}_4\text{C}$	27.32–27.44	27.38 (nr)	9
32	$\text{CC}_1\text{SS}$	27.32–27.44	27.38 (nr)	9
33	$\text{C}_4\text{SC}$	25.17	25.11	9
34	$\text{CC}_4\text{S}$	25.17	25.04	9
35	$\text{SSC}_4\text{S}$	25.17	25.04	<i>c</i>
36	$\text{CC}_4\text{VC}$	25.17	24.95	9
37	$\text{VC}_4\text{V}$	24.87	24.86	9

<sup>a</sup> The numbering and symbols are those indicated in Scheme 2.<sup>b</sup> Chemical shift values calculated by other authors (see the corresponding literature references) or by us in this work using the procedure explained in the text. <sup>c</sup> Calculated and experimental chemical shifts determined in this work.

firms that the T units are incorporated in the polymer chain. Moreover, the signals corresponding to  $\text{CST}_1$  (line 15) and  $\text{CVT}_1$  (line 16) suggest that the T units are followed by both vinyl monomers (V and S) and/or C units. However,  $^{13}\text{C}$  NMR signals corresponding to the  $\text{T}_4\text{S}$  and  $\text{T}_4\text{V}$  diads, expected at 30.4 and 30.6 ppm, are not detected in the spectra of these copolymers, even in samples rich in styrene. Assuming that these diads are oriented and that S and V insertion is secondary, this observation suggests that T units are formed exclusively after C units. If the last monomer inserted in the growing polymer chain is incorporated as a vinyl group (S or V), then the subsequently inserted monomer can only be a S, V, or C unit.

It has been suggested that in butadiene polymerizations catalyzed by half-sandwich titanocene compounds the preinsertion intermediate or the resting state of the catalyst is a  $\eta^3$ -allyl-Ti complex (Scheme 3) where the growing polymer chain is bound to the metal center in a syn or anti configuration.<sup>20</sup> When polymerization rate is rapid, the monomer insertion proceeds through the

**Scheme 2****Scheme 3**

anti intermediate, resulting in the formation of a *cis*-1,4 poly(butadiene) unit. Under these conditions, anti-syn isomerization of the allyl complex may occasionally occur, producing the syn intermediate, which in turn produces a *trans*-1,4 poly(butadiene) unit (Scheme 3).

Furthermore, coordination of the double bond of the penultimate unit in the growing polymer chain (backbiting) to the metal center of the active species stabilizes the catalyst in its resting state and assists monomer insertion. The observation that in the polymer chains of the sPS-B copolymers T units exclusively follow C units suggests that backbiting of the penultimate monomer unit likely assists the anti-syn isomerization of the  $\eta^3$ -allyl-Ti intermediate. When the penultimate unit is a vinyl monomer, coordination to the active metal center is less favorable, and butadiene insertion follows the pathway producing *cis*-1,4 units.

The  $^{13}\text{C}$  NMR assignments listed in Table 3 permitted the average styrene block lengths ( $n_s$ ) to be evaluated using eq 1.<sup>21</sup> The method used to calculate the  $n_s$  values is summarized in the Appendix.

The calculated  $n_s$  values for samples 11–18 are reported in Table 2. As expected from the reactivity ratios of the two monomers,<sup>11</sup> the molar fraction of the SB + BS diads is rather low compared to that of the BB and SS diads and reaches a maximum value in the copolymers that have a monomer composition close to 50 mol %. The average styrene block lengths increase with increasing styrene concentration in the copolymers. Sample 11, with the lowest styrene concentration ( $x_s = 0.15$ ), has an average block length of about six repeat units, which in principle could produce a crystalline polystyrene segment. Surprisingly, samples 11–14, which have styrene concentrations of up to  $x_s = 0.55$  and syndiotactic styrene block lengths of up to nine repeat units, did not exhibit a melting endotherm in the 200–270 °C range typical of crystalline syndiotactic

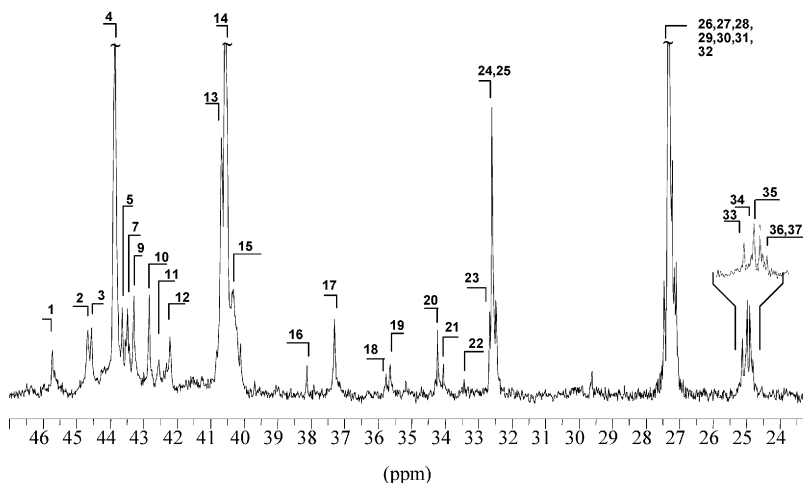


**Figure 1.** Aliphatic region of the  $^{13}\text{C}$  NMR spectrum (100.6 MHz for  $^{13}\text{C}$ ,  $\text{CDCl}_3$ , room temperature,  $\delta$  in ppm from TMS) of sample **15**. The numbering of the spectral lines is reported in Table 3.

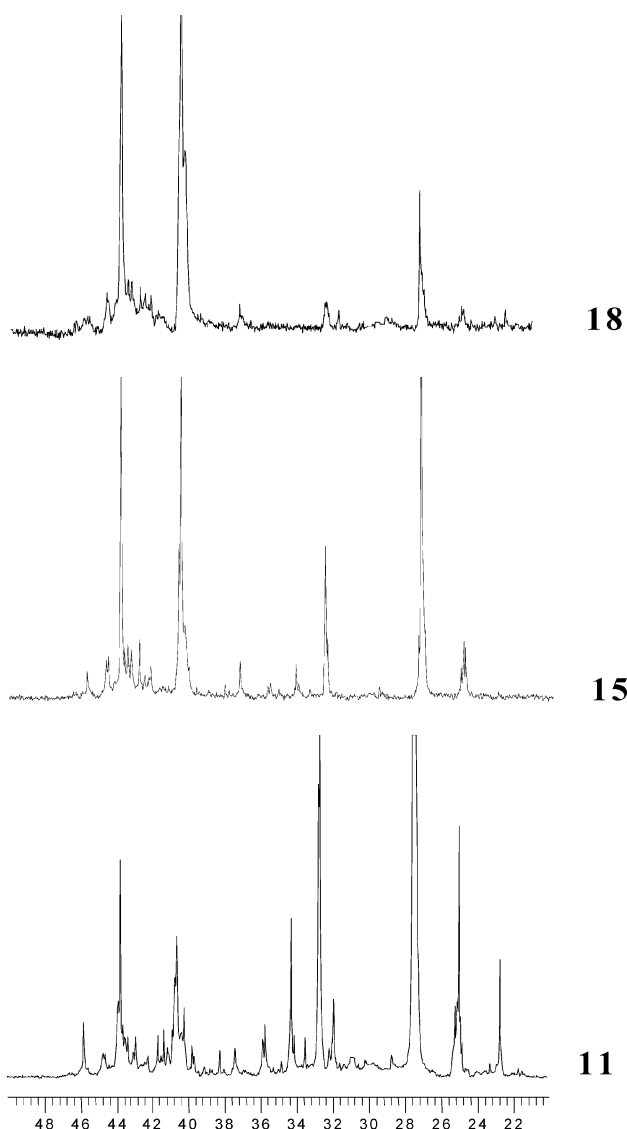


**Figure 2.** Aliphatic region of the  $^{13}\text{C}$  NMR spectrum (100.6 MHz for  $^{13}\text{C}$ ,  $\text{CDCl}_3$ , room temperature,  $\delta$  in ppm from TMS) of samples **11**, **15**, and **18**.

polystyrene by DSC, even in the first heating run. However, glass transitions were observed for the PBD segments (sample **11**,  $T_g = -95^\circ\text{C}$ ; sample **14**,  $T_g = -80$

$^\circ\text{C}$ ). Annealing the samples at  $130^\circ\text{C}$  for 1 h did not induce crystallization of the sPS homosequences. However, melting points were observed in copolymer samples with styrene molar fractions of  $x_S > 0.65$  (samples **15**–**18**). Melting points in the range  $205$ – $230^\circ\text{C}$  were observed without annealing, indicating that the crude material had crystalline syndiotactic polystyrene blocks. When these samples were annealed, there was no change in the melting point, indicating no additional crystallization with thermal treatment. The  $T_g$ 's for the PBD segments of these samples were not clearly detected. These results indicate that short syndiotactic polystyrene blocks are not crystalline and that the rate of crystallization is slow even with annealing at temperatures above the  $T_g$  of the syndiotactic styrene homosequences.

**sPS–B Copolymer Morphology.** Syndiotactic polystyrene has been observed in four crystalline forms, known in the literature as  $\alpha$ ,  $\beta$ ,  $\gamma$ , and  $\delta$ .<sup>22</sup> The  $\alpha$  and  $\beta$  forms consist of a “zigzag” or “all-trans” chain conformation,<sup>23</sup> whereas the  $\gamma$  and  $\delta$  forms are in the  $2(2/1)$  helix conformation.<sup>22,24</sup> The polymorphic behavior of sPS is further complicated by the fact that when the  $\alpha$ ,  $\gamma$ , and  $\delta$  crystalline forms are treated with THF, halogenated, and/or aromatic solvents, clathrated forms of these solvents are produced.<sup>22,23,25</sup> sPS homopolymers that are synthesized in or recovered from toluene are typically obtained in the toluene  $\delta$  clathrate form. Since the chemical, physical, and mechanical properties of sPS–B copolymers are influenced by the crystalline form of the sPS component, we first investigated this issue by X-ray powder diffraction (WAXD) and solid-state CP-MAS  $^{13}\text{C}$  NMR spectroscopy.

Samples **15**–**18** with  $x_S > 0.65$  and  $n_S$  in the range of 12–50 repeat units possessed crystalline sPS segments with melting points in the range  $205$ – $230^\circ\text{C}$ . The WAXD spectra of these samples (Figure 3) show that the native crystalline phase of these samples is the toluene- $\delta$  clathrate form characterized by signal at  $2\theta = 7.9^\circ$ ,  $10.1^\circ$ ,  $17.3^\circ$ ,  $20.0^\circ$ ,  $23.2^\circ$ , and  $27.2^\circ$ . The CP-MAS  $^{13}\text{C}$  NMR analysis of samples **15** and **18** confirms this result. The features observed in the cross-polarization–magic angle spinning  $^{13}\text{C}$  NMR (CP-MAS  $^{13}\text{C}$  NMR) spectra of sPS–B samples are identical to the features observed for crystalline sPS in the  $\delta$ -form (Figure 4).<sup>26</sup> The  $^{13}\text{C}$  signals corresponding to the PBD blocks appear less intense than expected on the basis of the chemical

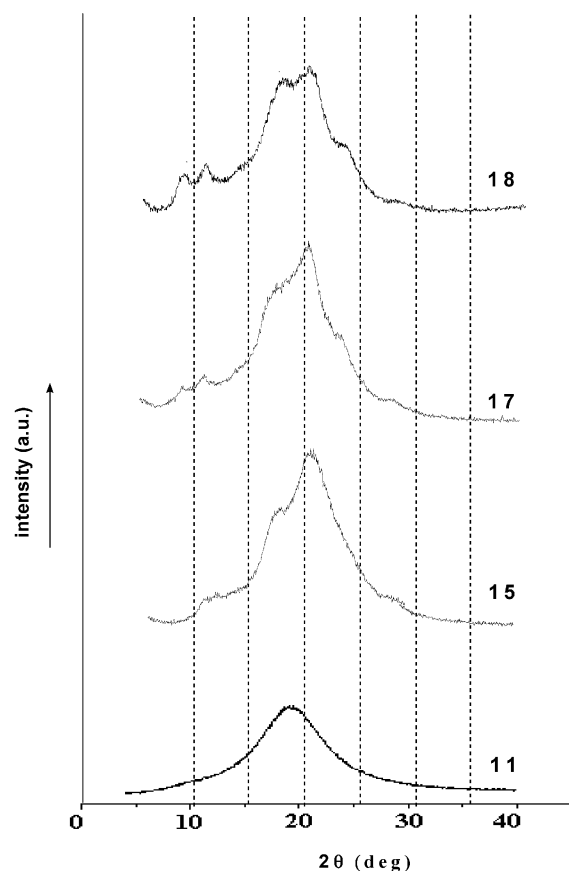


**Figure 3.** WAXD spectra of samples **11**, **15**, **17**, and **18**.

composition of the sample. This is likely to be due to the higher mobility of these chain segments and resulting loss of intensity during cross-polarization time of the acquisition pulse sequence.<sup>27</sup> The crystallinity of the samples decreases as the amount of sPS in the copolymer decreases. The X-ray reflections of the crystalline sPS disappear in the halo of the amorphous sPS when the styrene composition is lower than 50 mol % and styrene block lengths are shorter than nine repeat units. However, the polystyrene segments in samples with lower styrene content (**11**–**14**) still possess syndiotacticity but are simply in the amorphous clathrate form. The solid-state CP MAS <sup>13</sup>C NMR spectra of these samples exhibit signals at 42.5 and 145.5 ppm, which correspond to the methylene and ipso carbons of styrene units in a syndiotactic segment, respectively. The CP MAS spectrum of sample **11** shows the typical pattern expected for methylene carbons in a helical conformation of sPS in its amorphous clathrate form.<sup>26</sup> Annealing this samples for 1 h at 130 °C does not induce the crystallization of the syndiotactic styrene segments, which are either not observed or are amorphous by DSC and WAXD analysis. Conversely, annealing sample **18** for 1 h at 130 °C induces a transformation from the native  $\delta$ -toluene clathrate form observed in the uncured sample to the  $\gamma$ -form. The WAXD spectrum of the annealed sample **18** exhibits reflections at  $2\theta = 9.3^\circ$ ,  $10.4^\circ$ ,  $16.1^\circ$ , and  $19.9^\circ$  (Figure 5), which were previously assigned to the  $\gamma$ -form produced from the  $\delta$ -toluene clathrate form under similar conditions.<sup>22</sup> Thus, the sPS segments of sPS–B copolymers behave similarly to sPS homopolymer.

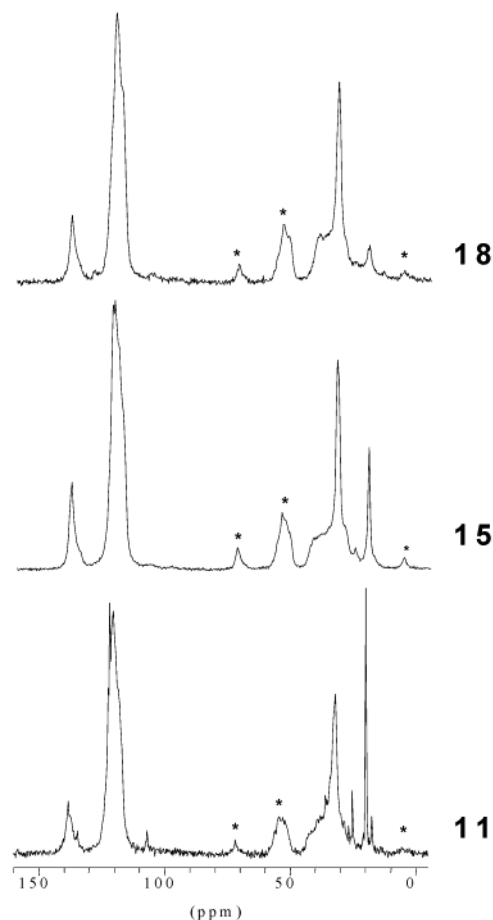


**Figure 4.** <sup>13</sup>C CP MAS NMR (75.4 MHz for <sup>13</sup>C, room temperature,  $\delta$  in ppm from TMS) spectra of samples **11**, **15**, and **18**. The peaks labeled with an asterisk are spinning sidebands.

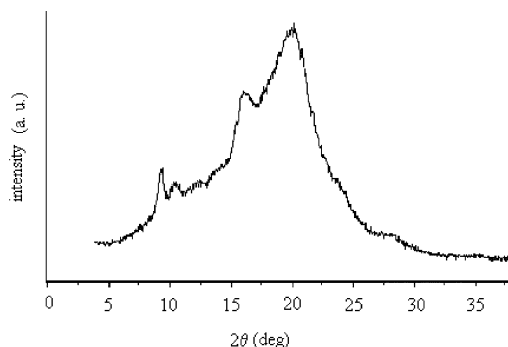


**Figure 5.** WAXD spectra of sample **18** after annealing at 130 °C for 1 h.

To better understand the fundamental relationship between the microstructure and morphology of sPS–B copolymers, sample **13** was analyzed by TEM (Figure 6). The micrograph shows an extensive network of long, thin styrenic fibers. In many cases the fibers are much longer than 100 nm and have diameters significantly less than 10 nm. Sample **13** has a relatively short syndiotactic styrene homosequence block length ( $n_S = 8.8$ ). The formation of fibers may be a result of the restricted mobility expected for an  $(AB)_n$  copolymer containing short random blocks. The result is small imperfect styrene domains that results amorphous at DSC analysis. The restricted mobility of the syndiotactic styrene blocks may also explain why annealing did not increase the copolymer crystallinity.



**Figure 6.** TEM micrograph of sample **13** ( $x_S = 0.37$ ;  $n_S = 8.8$ ).

The observed fibers consisting of phase-separated syndiotactic styrene homosequences should be highly reinforcing and improve the mechanical properties compared to those of a random anionic SBR of similar styrene content and butadiene homosequence microstructure. The mechanical properties of sPS–B copolymer are currently under investigation.

## Conclusions

Samples of sPS–B covering the full range of monomer compositions were prepared using  $\text{CpTiCl}_3/\text{MAO}$  at 25 °C. The composition of the feed stream was carefully calibrated in order to find a butadiene concentration in the feed stream suitable for the synthesis of a block copolymer. The  $^{13}\text{C}$  NMR analysis of the microstructure of these copolymers permitted the signals diagnostic of the monomer triads comprising the styrene unit to be assigned and the average block lengths of the styrene segments to be determined. Samples with  $n_S$  from 6 to 9 were completely amorphous with  $T_g$  values of the PBD segments in the range  $-95$  to  $-80$  °C. Thermal treatment of these samples above the  $T_g$  of atactic poly(styrene) does not induce crystallization of the syndiotactic styrene segments. The TEM micrograph of sample **13** ( $x_S = 0.37$  and  $n_S = 8.8$ ) shows an extensive network of long, thin styrenic fibers. In many cases the fibers are much longer than 100 nm and have diameters significantly less than 10 nm. The formation of fibers may be a result of the restricted mobility expected for an  $(\text{AB})_n$  copolymer containing short random blocks that results in small imperfect styrene domains.

Samples containing long syndiotactic styrene sequences ( $x_S > 0.65$  and  $n_S > 12$ ) exhibit crystalline domains consisting of syndiotactic polystyrene observed in the  $\delta$ -toluene clathrate form. As previously observed for pure sPS,<sup>22</sup> annealing at 130 °C for 1 h converts the sPS  $\delta$ -crystalline form into the corresponding  $\gamma$ -form. These results suggest that the sPS crystalline domains of the sPS–B copolymers can be modified in a fashion similar to sPS, producing materials with different properties.

## Experimental Section

**General Procedures and Materials.** All manipulations were performed under a nitrogen atmosphere using standard Schlenk techniques or an MBraun inert atmosphere drybox. Commercial grade toluene (Carlo Erba, 99.5%) was treated with sulfuric acid, washed with saturated bicarbonate solution and water, dried over calcium chloride, and distilled over sodium. Styrene (Aldrich) was purified by distillation at

reduced pressure over calcium hydride and stored at  $-20$  °C. Polymerization grade 1,3-butadiene, purchased from Società Ossigeno Napoli (SON, 99.5%) was dried by column passing over 3A molecular sieves activated at 200 °C in vacuo for 24 h.  $\text{CpTiCl}_3$  and MAO (10% w/w toluene solution) were purchased from Aldrich and used as received.

**Synthetic Procedure for sPS–B.** The sPS–B samples were prepared according to the following typical example (sample **18** of Table 2). A 1 L BUCHI glass autoclave equipped with a mechanical stirrer was charged with toluene (100 mL), styrene (50 mL), and MAO (0.6 g). The solution was stirred at 25 °C for 15 min, allowing the system to reach thermal equilibrium. A gas mixture with a composition of 2% v/v of butadiene in nitrogen was then allowed to flow through the reactor at a rate of 700 mL/min for 30 min. The polymerization was initiated by injecting of the desired amount of  $\text{CpTiCl}_3$  (6 mg,  $3 \times 10^{-5}$  mol, Al/Ti molar ratio = 400) dissolved in toluene (2 mL). The polymerization was terminated after 1 h by introducing ethanol (15 mL) containing the antioxidant (Wingstay K; 0.5–0.75 parts by weight). The copolymer was coagulated in ethanol (200 mL) acidified with aqueous HCl, recovered by filtration, washed with an excess of fresh ethanol, and dried in vacuo at room temperature until a constant weight was achieved. The yield was 1.25 g ( $M_w = 26\,000$ ;  $M_w/M_n = 2.6$ ). The butadiene/nitrogen gas mixture was calibrated using the following method. Gaseous butadiene was passed through a column of dried silica and mixed with pure nitrogen using a Brooks gas flow meter. Samples of the gaseous mixture going to and coming from the autoclave were collected and analyzed by GC. The relative concentrations were compared to a calibration curve prepared using butadiene samples of known concentration. Typically, butadiene concentrations were in the 2–16% v/v range. A correlation was made between the butadiene concentration in the gas phase and in toluene solutions under the polymerization conditions, thus allowing the molar fraction of butadiene in solution during the polymerization runs to be determined.

**Gel Permeation Chromatography (GPC).** The average molecular weights of the copolymer samples were determined at 30 °C with a 150C Waters GPC equipped with JASCO 875-UV (254 nm) and WGE-DR BURES ETA1002 refractive index detectors and three PSS columns set consisting of  $10^5$ ,  $10^4$ , and 100 Å (pore size)–5  $\mu\text{m}$  (particle size) column.  $\text{CHCl}_3$  was the carrier solvent used with a flow rate of 1.0 mL/min. The calibration curve was established with polystyrene standards.

**Differential Scanning Calorimetry (DSC).** DSC measurements were carried out on Mettler calorimeter at a heating rate of 10 °C/min.

**X-ray Analysis.** Wide-angle X-ray diffraction (WAXD) patterns in the range  $2\theta = 4^\circ$ – $40^\circ$  were obtained with an automatic Philips instrument using the nickel-filtered  $\text{Cu K}\alpha$  radiation.

**TEM Analysis.** Copolymers were sectioned to approximately 70 nm thickness using a cryoultramicrotome, supported on 3 mm copper grids, and stained with osmium tetroxide. Samples were then examined with a Philips EM400 transmission electron microscope operating at 100 kV.

**Solution  $^1\text{H}$  NMR and  $^{13}\text{C}$  NMR Analysis.** The copolymer samples (25 mg) were dissolved in chloroform- $d_1$  (0.4 mL, 20 wt %) in a 5 mm (o.d.) NMR tube and analyzed at room temperature with a Bruker AVANCE 400 spectrometer (400 MHz for  $^1\text{H}$  and 100 MHz for  $^{13}\text{C}$ ). NMR chemical shifts are reported in ppm and referenced to TMS. The monomer compositions of samples **1–18** were determined by comparing the integrals of the following  $^1\text{H}$  resonances ( $\delta$  in ppm,  $\text{CDCl}_3$ , 25 °C): 7.07 and 6.56 (5H, m,  $\text{CH}_2\text{CH}(\text{C}_6\text{H}_5)$ ); 5.58 (1H, m,  $\text{CH}_2\text{-CH}_2(\text{CH}=\text{CH}_2)$ ); 5.38 (2H, m,  $\text{CH}_2\text{CH}=\text{CHCH}_2$ ). The following  $^{13}\text{C}$  NMR acquisition parameters were used: relaxation delay between scans = 2 s; acquisition time = 0.34 s; flip angle =  $45^\circ$  (corresponding to 2  $\mu\text{s}$ ); number of transients = 20K; WALTZ-16 pulse sequence for the  $^1\text{H}$  decoupling.

**Solid-State CP-MAS  $^{13}\text{C}$  NMR.** Solid-state  $^{13}\text{C}$  NMR spectra were recorded on a Bruker AVANCE 300 spectrometer (300 MHz for  $^1\text{H}$  and 75.4 MHz for  $^{13}\text{C}$ ). Copolymer samples (ca. 250 mg) were charged in a zirconia rotor (o.d. 4 mm) and



spun at 5000 Hz at the magic angle. The cross-polarization method with high-power decoupling was employed for generating the  $^{13}\text{C}$  signal. The following acquisition parameters were used: relaxation delay between scans = 2 s; spin locking time = 2 ms; number of transients = 1K. The chemical shifts are referenced to TMS and determined using the peak of crystalline polyethylene at 33.4 ppm as internal reference.

**Acknowledgment.** This work was supported by the The Goodyear Tire & Rubber Co., Italian National Research Council (CNR), and MURST (Ministero dell'Università e della Ricerca Scientifica, Roma, Italy; PRIN-2000: "Polimerizzazione selettiva: catalizzatori di coordinazione e controllo delle proprietà fisiche dei polimeri risultanti").

## Appendix

The  $n_s$  values were calculated according to eq 1 conventionally used to evaluate the average block lengths on the basis of monomer triads.<sup>21</sup> It is worth mentioning that, as explained in the text, the triads are in this case oriented and the asymmetric triad BSS is not equivalent to SSB.

$$n_s = \frac{\text{SSS} + \text{BSS} + \text{SSB} + \text{BSB}}{\text{BSB} + \frac{1}{2}(\text{BSS} + \text{SSB})} \quad (1)$$

The molar concentrations of the different triads were assumed to be proportional to the integrals of the  $^{13}\text{C}$  NMR spectral lines indicated in the following equations (the numbering of the signals is that reported in Table 3):

$$\text{BSS} = \text{CSS} + \text{VSS} + \text{TSS} = 17 + 12$$

$$\text{SSB} = \text{SSC} + \text{SSV} + \text{SST} = 7 + 12$$

$$\begin{aligned} \text{BSB} &= \text{CSC} + \\ &(\text{VSV} + \text{CST} + \text{CSV} + \text{VSC} + \text{VST}) = 1 \\ \text{SSS} &= 14 \end{aligned}$$

The sequences written in italics, namely TSS, TST, TSC, and TSV, were omitted in the calculations because the TS diad is not observed in the copolymers (infra the text). The sequences VSV, CST, CSV, VSC, and VST were considered negligible with respect to the CSC triad.

## References and Notes

- (1) (a) Henderson, J. N. *Styrene Butadiene Rubbers*. In *Rubber Technology*, 3rd ed.; Chapman & Hall: London, 1995; p 209 ff and references reported therein. (b) Bates, F. S.; Berney, C. V.; Cohen, R. E. *Macromolecules* **1983**, *16*, 1101. (c) Bates, F. S.; Berney, C. V.; Cohen, R. E. *Polymer* **1983**, *24*, 519. (d) Storey, R. F.; George, S. E.; Nelson, M. E. *Macromolecules* **1991**, *24*, 2920. (e) Winey, K. I.; Thomas, E. L.; Fetters, L. J. *Macromolecules* **1992**, *25*, 422. (f) Quirk, R. P.; Ma, J.-J. *Polym. Int.* **1991**, *24*, 197.
- (2) Molau, G. E. In *Block Polymers*; Aggarwal, S. L., Ed.; Plenum Press: New York, 1970; p 79 ff.
- (3) (a) Gallot, B. R. M. *Adv. Polym. Sci.* **1978**, *29*, 85. (b) Folkes, M. J., Ed.; *Processing, Structure and Properties of Block Copolymers*; Elsevier Applied Science: New York, 1985. (c) Quirk, R. P.; Kinning, D. J.; Fetters, L. J. In *Comprehensive Polymer Science*; Aggarwal, S. L., Ed.; Pergamon Press: Oxford, U.K., 1989; Vol. 7, p 1. (d) Bates, F. S.; Fredrickson, G. H. *Annu. Rev. Phys. Chem.* **1990**, *41*, 525.
- (4) (a) Bradford, E. B.; Vanzo, E. *J. Polym. Sci., Part A1* **1968**, *6*, 1661. (b) Lewis, P. R.; Price, C. *Polymer* **1972**, *13*, 20. (c) Bi, L. K.; Fetters, L. J. *Macromolecules* **1975**, *8*, 98. (d) Odell, J. A.; Dlugosz, J.; Keller, A. *J. Polym. Sci., Polym. Phys. Ed.* **1976**, *14*, 861.
- (5) (a) Holden, G.; Milkovich, R. Belgian Patent 627,652, July 29, 1963; U.S. Patent 3,265,765, August 9, 1965, filed January 29, 1962. (b) Holden, G.; Bishop, E. T.; Legge, N. R. *Proceedings of the International Rubber Conference, 1967*; MacLaren and Sons: London, 1968; p 287; *J. Polym. Sci., Part C* **1969**, *26*, 37.
- (6) Kennedy, J. P. *Thermoplastic Elastomers by Carbocationic Polymerization*. In *Thermoplastic Elastomers*; Holden, G., Legge, N. R., Quirk, R., Schroeder, H. E., Eds.; Hanser: Cincinnati, OH, 1999; p 48.
- (7) Holden, G.; Legge, N. R. *Styrenic Thermoplastic Elastomers*. In *Thermoplastic Elastomers*; Holden, G., Legge, N. R., Quirk, R., Schroeder, H. E., Eds.; Hanser: Cincinnati, OH, 1999; p 382.
- (8) (a) Katrizky, A. R.; Weiss, D. E. *J. Chem. Soc., Chem. Commun.* **1974**, 401. (b) Katrizky, A. R.; Weiss, D. E. *J. Chem. Soc., Perkin Trans.* **1975**, 21.
- (9) (a) Segre, A. L.; Delfini, M.; Conti, F.; Boicelli, A. *Polymer* **1975**, *16*, 338. (b) Conti, F.; Delfini, M.; Segre, A. L. *Polymer* **1977**, *18*, 310.
- (10) Sato, H.; Ishikawa, T.; Takebayashi, K.; Tanaka, Y. *Macromolecules* **1989**, *22*, 1748.
- (11) (a) Zambelli, A.; Grassi, A.; Caprio, M.; Bowen, D. E. Syndiotactic Styrene-Butadiene Block Copolymer and Its Manufacture. Eur. Pat. Appl. EP 1013683, 2000. (b) Zambelli, A.; Caprio, M.; Grassi, A.; Bowen, D. E. *Macromol. Chem. Phys.* **2000**, *201*, 393.
- (12) Bywater, S. *Polym. Commun.* **1983**, *24*, 203. (b) Sato, H.; Takebayashi, K.; Tanaka, Y. *Macromolecules* **1987**, *20*, 2418.
- (13) (a) Pellicchia, C.; Pappalardo, D.; Oliva, L.; Zambelli, A. *J. Am. Chem. Soc.* **1995**, *117*, 6593. (b) Grassi, A.; Zambelli, A.; Laschi, F. *Organometallics* **1996**, *15*, 480. (c) Grassi, A.; Saccheo, S.; Zambelli, A.; Laschi, F. *Macromolecules* **1998**, *31*, 5588. (d) Pellicchia, C.; Grassi, A. *Top. Catal.* **1999**, *7*, 125.
- (14) (a) Ricci, G.; Italia, S.; Giarrusso, A.; Porri, L. *J. Organomet. Chem.* **1993**, *451*, 67.
- (15) Grassi, A.; Caprio, M.; Zambelli, A.; Bowen, D. E. *Macromolecules* **2000**, *33*, 8130.
- (16) (a) Ishihara, N.; Seimiya, T.; Kuramoto, M.; Uoi, M. *Macromolecules* **1986**, *19*, 2464. (b) Ishihara, N.; Kuramoto, M.; Uoi, M. *Macromolecules* **1988**, *21*, 3356.
- (17) Beebe, D. H. Goodyear Tire & Rubber Co., Akron, OH, personal communication.
- (18) Van der Velden, G.; Didden, C.; Veermans, T.; Beulen, J. *Macromolecules* **1987**, *20*, 1252.
- (19) Kakuta, K.; Tamai, H.; Wong, P.-H.; Kawahara, S.; Tanaka, Y. *Macromolecules* **1999**, *32*, 5994.
- (20) (a) Porri, L.; Giarrusso, A. In *Comprehensive Polymer Science*; Eastmond, G. C., Ledwith, A., Russo, S., Sigwalt, P., Eds.; Pergamon Press: Oxford, U.K., 1989; Vol. 4, Part II, p 53. (b) Porri, L.; Giarrusso, A.; Ricci, C. *Prog. Polym. Sci.* **1991**, *16*, 405. (c) Porri, L.; Giarrusso, A.; Ricci, C. *J. Polym. Sci., Part A* **1994**, *36*, 1421. (d) Guerra, G.; Cavallo, L.; Corradini, P.; Fusco, R. *Macromolecules* **1997**, *30*, 677. (e) Peluso, A.; Improta, R.; Zambelli, A. *Macromolecules* **1997**, *30*, 2219. (f) Costabile, C.; Milano, G.; Cavallo, L.; Guerra, G. *Macromolecules* **2001**, *34*, 7952.
- (21) Randall, J. C. *J. Macromol. Sci., Rev. Macromol. Chem. Phys.* **1989**, *C29* (2&3), 29.
- (22) Guerra, G.; Vitagliano, M.; De Rosa, C.; Petraccone, V.; Corradini, P. *Macromolecules* **1990**, *23*, 1539.
- (23) (a) Immirzi, A.; De Candia, F.; Iannelli, P.; Vittoria, V.; Zambelli, A. *Makromol. Chem., Rapid Commun.* **1988**, *9*, 761. (b) Vittoria, V.; Russo, R.; De Candia, F. *Polymer* **1991**, *32*, 337. (c) De Rosa, C.; Rapacciuolo, M.; Guerra, G.; Petraccone, V.; Corradini, P. *Polymer* **1992**, *33*, 1423. (d) Guerra, G.; De Rosa, C.; Vitagliano, V. M.; Petraccone, V.; Corradini, P. *Polym. Commun.* **1991**, *32*, 30.
- (24) Corradini, P.; Napoletano, R.; Pirozzi, B. *Eur. Polym. J.* **1990**, *26*, 157.
- (25) (a) Chatani, Y.; Shimane, Y.; Inoue, Y.; Inagaki, T.; Ishioka, T.; Ijitsu, T.; Yukinari, T. *Polymer* **1992**, *33*, 488. (b) Chatani, Y.; Shimane, Y.; Inagaki, T.; Ijitsu, T.; Yukinari, T.; Shikuma, H. *Polymer* **1993**, *34*, 1620. (c) Chatani, Y.; Inagaki, T.; Shimane, Y.; Shikuma, H. *Polymer* **1993**, *34*, 4841.
- (26) (a) Grassi, A.; Longo, P.; Guerra, G. *Makromol. Chem., Rapid Commun.* **1989**, *10*, 687. (b) Gomez, M. A.; Tonelli, A. E. *Macromolecules* **1991**, *24*, 3533.
- (27) Fyfe, C. A. *Solid State NMR for Chemists* CFC Press: Guelph, Ontario, Canada, 1983.